NASA/TM-20205003857

In-Situ Alloying of GRCop-42 via Additive Manufacturing: Precipitate Analysis

David S. Scannapieco and John J. Lewandowski
Case Western Reserve University, Cleveland, Ohio

Richard B. Rogers and David L. Ellis
Glenn Research Center, Cleveland, Ohio

August 2020

NASA STI Program . . . in Profile

Since its founding, NASA has been dedicated to the advancement of aeronautics and space science. The NASA Scientific and Technical Information (STI) Program plays a key part in helping NASA maintain this important role.

The NASA STI Program operates under the auspices of the Agency Chief Information Officer. It collects, organizes, provides for archiving, and disseminates NASA's STI. The NASA STI Program provides access to the NASA Technical Report Server—Registered (NTRS Reg) and NASA Technical Report Server—Public (NTRS) thus providing one of the largest collections of aeronautical and space science STI in the world. Results are published in both non-NASA channels and by NASA in the NASA STI Report Series, which includes the following report types:

- TECHNICAL PUBLICATION. Reports of completed research or a major significant phase of research that present the results of NASA programs and include extensive data or theoretical analysis. Includes compilations of significant scientific and technical data and information deemed to be of continuing reference value. NASA counter-part of peer-reviewed formal professional papers, but has less stringent limitations on manuscript length and extent of graphic presentations.

- TECHNICAL MEMORANDUM. Scientific and technical findings that are preliminary or of specialized interest, e.g., "quick-release" reports, working papers, and bibliographies that contain minimal annotation. Does not contain extensive analysis.

- CONTRACTOR REPORT. Scientific and technical findings by NASA-sponsored contractors and grantees.

- CONFERENCE PUBLICATION. Collected papers from scientific and technical conferences, symposia, seminars, or other meetings sponsored or co-sponsored by NASA.

- SPECIAL PUBLICATION. Scientific, technical, or historical information from NASA programs, projects, and missions, often concerned with subjects having substantial public interest.

- TECHNICAL TRANSLATION. English-language translations of foreign scientific and technical material pertinent to NASA's mission.

For more information about the NASA STI program, see the following:

- Access the NASA STI program home page at http://www.sti.nasa.gov

- E-mail your question to help@sti.nasa.gov

- Fax your question to the NASA STI Information Desk at 757-864-6500

- Telephone the NASA STI Information Desk at 757-864-9658

- Write to:
  NASA STI Program
  Mail Stop 148
  NASA Langley Research Center
  Hampton, VA 23681-2199

NASA/TM-20205003857

In-Situ Alloying of GRCop-42 via Additive Manufacturing: Precipitate Analysis

David S. Scannapieco and John J. Lewandowski
Case Western Reserve University, Cleveland, Ohio

Richard B. Rogers and David L. Ellis
Glenn Research Center, Cleveland, Ohio

National Aeronautics and
Space Administration

Glenn Research Center
Cleveland, Ohio 44135

August 2020

Acknowledgments

Thanks to Dereck Johnson, Aaron Thompson, Wayne Jennings, Joy Buehler, Laura Evans, Pete Bonacuse, and Cheryl Bowman of NASA Glenn Research Center and Paul Gradl, Chris Protz, and John Fikes of NASA Marshall Space Flight Center for their support and advisement on this work. This work was supported by NASA's Rapid Analysis and Manufacturing Propulsion Technology (RAMPT) Program under grant number 80NSSC19K1736. Professor John J. Lewandowski was also supported by the Arthur P. Armington Professorship at Case Western Reserve University.

This report is a formal draft or working paper, intended to solicit comments and ideas from a technical peer group.

This report contains preliminary findings, subject to revision as analysis proceeds.

Level of Review: This material has been technically reviewed by technical management.

Available from

NASA STI Program
Mail Stop 148
NASA Langley Research Center
Hampton, VA 23681-2199

National Technical Information Service
5285 Port Royal Road
Springfield, VA 22161
703-605-6000

This report is available in electronic form at http://www.sti.nasa.gov/ and http://ntrs.nasa.gov/

In-Situ Alloying of GRCop-42 via Additive Manufacturing: Precipitate Analysis

David S. Scannapieco and John J. Lewandowski
Case Western Reserve University
Cleveland, Ohio 44106

Richard B. Rogers and David L. Ellis
National Aeronautics and Space Administration
Glenn Research Center
Cleveland, Ohio 44135

Abstract

In situ alloying of elemental Cu, Cr, and Nb to form GRCop-42 (Cu-4at.% Cr-2at.% Nb) using laser powder bed fusion (LPBF) additive manufacturing (AM) was successful. Evaluation of the in situ alloyed GRCop-42 (ISGRCop-42) was conducted using phase extraction to explore the effects of AM process conditions on the formation of Cr_2Nb precipitates from elemental powders. It was found that ISGRCop-42 successfully and repeatedly formed Cr_2Nb at a yield as high as 89% of potential Cr_2Nb content. Initial work shows that powder preparation was the most influential factor in alloying success, followed by laser power.

Introduction

GRCop-42, a Cu-4 at.% Cr-2 at.% Nb alloy, was designed for high temperature mechanical properties and high thermal conductivity (Refs. 1 and 2). The GRCop alloy family has a nearly pure Cu matrix with Cr_2Nb precipitates that provide dispersion strengthening. The nearly pure matrix of Cu allows for high thermal conductivity while the precipitates contribute high temperature mechanical properties to make the alloy viable in combustion chambers (Ref. 1). GRCop alloys require high cooling rates during solidification because the formation of Cr_2Nb occurs rapidly when below the liquidus temperature of the compound. Historically, this alloy has been made by gas atomization for conventional manufacturing techniques. Gas atomization typically has cooling rates in the 10^4 K/s range (Refs. 2 and 3). This process creates pre-alloyed powders containing Cr_2Nb precipitates that are then consolidated via HIP, extrusion, etc.

However, laser-based AM processes can produce cooling rates between 10^4 K/s and 10^6 K/s (Ref. 4) while also providing more design freedom, finer details, and better yield than conventional processing techniques. Recent work has used pre-alloyed powders for AM to produce GRCop rocket engine combustion chambers (Ref. 5). Further exploration of the capabilities of AM, with the goal of in-situ alloying with elemental powders, is desired to reduce cost and quickly tailor alloy properties within a component to optimize performance. In addition, AM processes may provide small-batch explorations into new alloys for improved material capabilities across industries.

The high cooling rates of AM suggest it may be possible to use elemental powders to form Cr_2Nb in situ while fabricating components with similar properties as those produced using gas atomized GRCop powders. This work explores the effects of different elemental powder preparations and printing parameters on the formation of Cr_2Nb using LPBF.

Experimental Procedures

Elemental powders were acquired from American Elements. The copper powder was 10 to 50 μm in diameter, typical for LPBF processing. The niobium powder came in two lots, both of which were under 10 μm in size. The chromium also came in two lots. The first lot had a diameter range of 30 to 100 μm with a mean particle diameter greater than 50 μm, and the second lot was finer than 10 μm. Due to the eventual focus on milling of just Cr and Nb and the small proportion needed for GRCop-42 (~7 vol% combined Cr and Nb), the powder runs used in the builds can be considered to follow the Cu powder flow and size metrics, which are purchased specifically for LPBF.

Powders for LPBF builds were prepared by a combination of high energy ball milling and rolling to achieve uniform spatial distributions of Cr and Nb in the Cu. A schematic of the preparation process for each build is shown in Figure 1. As of the writing of this report, Builds 1 through 10 have been completed. To get an idea of impacts of parameter sets on the alloying process, 11 specimens that represent the outer boundary of all parameter sets used were analyzed. The specimens and their normalized milling and printing parameters are summarized in Table 1.

All milling was conducted with 6.6 mm stainless steel balls in stainless steel chambers backfilled with high purity Ar. Powders for Builds 1 and 3 were milled on a 4-position planetary mill and the Cu, first lot of Cr, and first lot of Nb were milled together. Build 5 milled the first lots of Cr and Nb together and then added Cu via rolling. The milling of Cr and Nb was done on a single position planetary mill with 6.6 mm stainless steel balls in a stainless steel chamber. Builds 7, 8, and 10 incorporated the same powder preparation process as build 5 but used the second lots of Cr and Nb powders of smaller size.

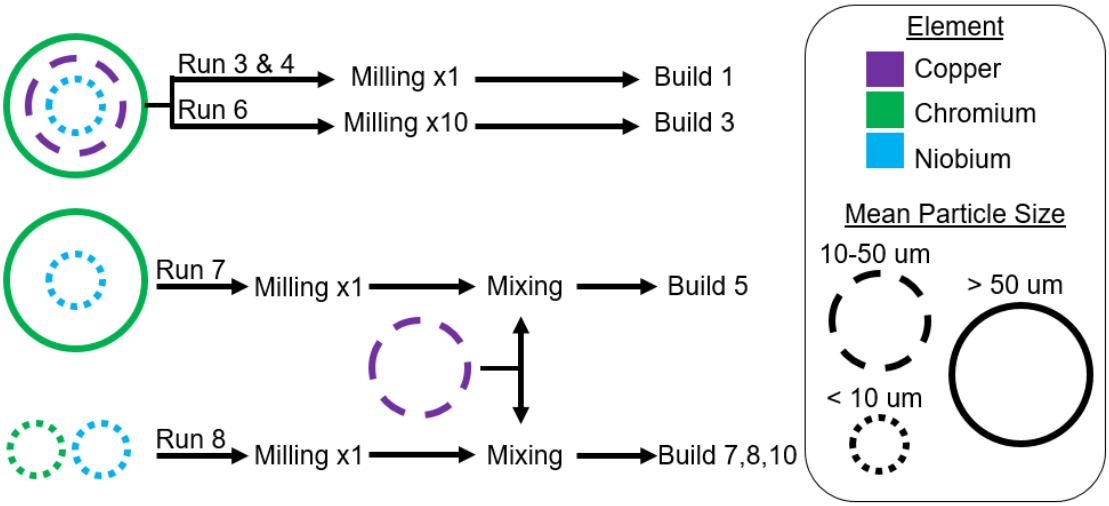

Figure 1.—Schematic of the powder preparation for builds analyzed.

TABLE 1.—NORMALIZED MILLING AND PRINTING PARAMETERS OF EACH SPECIMEN

Specimen	Power	Scan speed	Powder run	Cr+Nb Milled?	Milling time, τ	PBR	RPM
01F	0.50	1.00	3 & 4	No	1	5	115
01B	0.75	0.75	3 & 4	No	1	5	115
03J	1.54	0.39	6	No	10	5	115
05H	1.10	0.56	7	Yes	1	10	50
05P	1.10	0.25	7	Yes	1	10	50
05U	0.44	0.08	7	Yes	1	10	50
07AA	1.21	1.00	8	Yes	1	10	50
08C	1.25	1.25	8	Yes	1	10	50
10AJ	1.87	0.44	8	Yes	1	10	50
10AN	1.37	0.67	8	Yes	1	10	50
10AP	1.87	0.67	8	Yes	1	10	50

Once prepared, the powders were consolidated in an EOS M100 at NASA Glenn Research Center (GRC) utilizing a wide array of laser powers and scan speeds. The labeling scheme used in this report is [number][number][letter][letter] where the numbers are the build number and the letter(s) refer to a laser parameter set used to build the specimen, as described below.

To investigate build parameter effects on alloying, 1 cm cubes (Gao parameter blocks) were built using differing laser power and scan speed settings (Ref. 6). Data collected from x-ray diffraction (XRD) on a Bruker D8 ADVANCE with Cu K_α radiation showed that the Cu matrix (93 vol% of the material) dominated the detectors, eliminating any possibility for detailed examination of the precipitates. In an effort to increase the clarity of the data collected from the precipitates a phase extraction was conducted to remove the Cu matrix. The phase extraction allowed for detailed study of the precipitates phases as a result of the in situ process (Ref. 7).

For the phase extraction the parameter blocks were first sectioned to obtain samples with a mass of 0.617 to 1.900 g, which corresponds to volumes between 70 and 215 mm^3. These pieces were dissolved in 30 ml of nitric acid and the residue was vacuum filtered through a Buchner funnel with 0.450 μm filter paper. Best extractions were achieved using a mass between 1.2 and 1.5 g. These masses gathered a sufficient amount of precipitates but did not clog the filter paper. The precipitates that remained on the filter paper were scraped into sample jars using a razor. The amount of precipitates collected was between 0.0972 and 0.2471 g. These weights did not include losses during transfer. In addition to the ISGRCop extractions, an extraction was done on AM GRCop-42 (AMGRCop), made from conventionally gas atomized powders, for comparison between the precipitates of ISGRCop-42 and AMGRCop-42. The one specimen of AMGRCop was manufactured by a contractor for NASA Marshall Space Flight Center (MSFC) for the purposes of identifying AMGRCop-42 printing parameters similar to the work by Cooper, et al. (Ref. 5).

The extracted precipitates from all processing techniques were distributed onto individual single-crystal silicon wafers (low background holder) for XRD analysis. Scans were conducted in a Bruker D8 ADVANCE with Cu K_α radiation. Each scan traversed 2θ values of 10° to 120° at a step of 0.02°. Jade XRD analysis software was used to conduct the quantitative phase analysis on each sample using the whole pattern fitting (Rietveld refinement) method (Refs. 8 and 9). A common pattern fit file, based on Specimen 5U, was used for all of the samples. Specimen 5U was taken as the basis due to the presence of the Cu phase and its lack of a Cr-deficiency, discussed later.

Precipitates were mounted and examined in a Hitachi S4700 Scanning Electron Microscope (SEM) for morphological comparison between the ISGRCop-42 and AMGRCop-42. SEM and energy dispersive spectroscopy (EDS) was conducted at 15 keV and 15 μA under secondary electron imaging. With a density of 8.889 g/cm^3 (Ref. 2) interaction depth and volume interaction of the beam were estimated to be 0.653 μm and 0.520 μm^3, respectively (Ref. 10).

Results and Discussion

Table 2 shows the detected phases for each of the ISGRCop-42 specimens, the AMGRCop specimen, and the milled Cr and Nb (i.e., Cr + Nb) powder used for Builds 7, 8, and 10, which represents the starting elemental powders. (*) Note that the AMGRCop specimen has 97 wt% Cr_2Nb which is actually 88.2 wt% of the hexagonal, high-temperature Cr_2Nb phase and 8.8 wt% of the cubic, room-temperature Cr_2Nb phase. This dual-phase Cr_2Nb is not seen in any other specimen examined and for the purposes of in-situ alloying either phase is an acceptable outcome.

Only Nb-based oxides were present among the precipitates while no oxides were evident in the milled powder. This suggests that Nb-based oxides are forming during the extraction of LPBF, despite oxygen content below 0.1% during the printing process. Future work will investigate the source of the oxides and work to mitigate their presence. Some extractions ended prematurely as noted by the detectable level of Cu in specimens 01F and 05U.

TABLE 2.—PHASES DETECTED BY XRD (IN WEIGHT PERCENT)

Specimen	Cr_2Nb, percent	Cr, percent	Nb, percent	$NbO_{0.8}$, percent	NbO, percent	NbO_2, percent	Cu, percent
Cr+Nb	0.0	53.8	46.2	0.0	0.0	0.0	0.0
01F	14.7	3.3	58.7	2.0	2.4	5.1	13.8
01B	20.3	3.5	58.4	0.0	5.6	12.1	0.0
03J	15.6	1.0	55.1	0.0	16.3	12.1	0.0
05H	53.7	12.0	25.0	3.3	3.6	2.3	0.0
05P	71.3	6.1	7.4	2.7	8.6	3.8	0.0
05U	38.5	24.3	18.0	3.5	1.4	3.5	10.8
07AA	70.3	8.6	12.3	0.0	5.9	2.9	0.0
08C	64.7	11.8	15.7	0.0	5.2	2.6	0.0
10AJ	67.1	5.6	3.1	0.0	18.0	6.2	0.0
10AN	75.4	6.8	7.6	0.0	6.8	3.4	0.0
10AP	63.2	6.6	10.5	0.0	15.7	3.9	0.0
AMGRCop	*97.0	0.0	0.0	0.0	0.0	3.0	0.0

*AMGRCop has 97 wt% Cr_2Nb which is 88.2 wt% hexagonal Cr_2Nb phase and 8.8 wt% cubic Cr_2Nb phase.

The Cr powder used in Builds 1 and 3 were in excess of 50 μm. The maximum usable powder diameter for the EOS M100 is about 60 μm. It was suspected that a significant proportion of the Cr was removed due to this upper powder size limit. Table 3 shows the atomic percentages of each element present in the precipitates based upon the XRD phase results and confirms a deficiency of Cr in specimens 01F, 01B, and 03J.

In Build 5, the same Cr and Nb powders were used but the powders were milled without Cu to reduce their size and improve physical contact between Cr and Nb in order to promote Cr_2Nb formation. Build 5 specimens did have a higher proportion of Cr_2Nb compared to all Builds 1 and 3 specimens.

To improve the alloying further, Builds 7, 8, and 10 used smaller Cr and Nb powders to further increase surface area contact between Cr and Nb. With this powder preparation an improvement in the consistency and success of the alloying process was obtained. The weight percent of converted Cr_2Nb ranged from 63 to 75 wt% for Builds 7, 8, and 10, which all used the same starting powder. This demonstrated more consistent alloying success as a result of the powder preparation, in contrast to Build 5 that generated Cr_2Nb in the range from 38 to 71 wt%. Furthermore, the Nb proportion was consistent within each of the Builds 7, 8, and 10 specimens, while in Build 5 the Nb content ranged from 29 to 41 at.%. The Cr in Builds 7, 8, and 10 also only varied by 11 at.%, as seen in Table 3.

To analyze the impact of laser parameters on alloying the results were normalized by taking the amount of Cr in the Cr_2Nb phase as a proportion of the total Cr found in each sample. A similar procedure was conducted to identify the proportion of Nb in the Cr_2Nb. The results are shown in the last two columns of Table 3. This method allowed for quantification of how well the laser parameters promoted alloying while taking into account the impact of Cr deficiencies found in earlier builds.

Figure 2 shows the alloying efficiency (i.e., conversion to Cr_2Nb) with respect to the laser power and scan speed. Both laser parameters are normalized to the parameters of specimen 01A, which is not reported on in this study. Specimen 01A was chosen to be the standard because it was the first parameter block printed and there was a need to normalize parameters consistently within an ever expanding data set. Power comparisons show that there was a clear difference in samples below and above a normalized power of 1.1. A normalized laser power above 1.1 appeared to have higher alloying efficiency with higher consistency as well. The alloying efficiency appeared to asymptotically approach ~90% Cr in the Cr_2Nb phase. This might suggest that continuing to increase laser power is not an efficient method of improving alloying effectiveness in this process.

Figure 2 also shows the scan speed influence on alloying efficiency. In one analysis, all of the samples were included to compare the overall effect of scan speed. However, as noted previously, specimens printed with > 1.1 normalized power had higher alloying efficiency. This subset of samples was examined separately. There appears to be no correlation of scan speed with alloying efficiency as

shown by the R^2 value for all specimens in the scan speed versus Cr in Cr_2Nb plot being 0.0153, indicating little to no effect of the scan speed on proportion of Cr in Cr_2Nb. For the subset with normalized powers greater than 1.1, lower scan speeds improved alloying efficiency. This matches expectations, since increasing the dwell time provides more time for the Cr and Nb to react to form Cr_2Nb. While this trend appears to be linear, the slope of the regression line is quite small, indicating little influence of scan speed on alloying. This implies that changing the laser scan speed is unlikely to greatly influence the alloying efficiency of ISGRCop-42.

Specimens 10AN, 10AP, and AMGRCop were analyzed using the SEM to investigate differences in Cr_2Nb particle morphology caused by varying the build parameters. 10AP and 10AN were selected because they were amongst the higher and lower oxygen content specimens, respectively. Staying within the same build, powder preparation variables are eliminated and the chemical influences on precipitates could be isolated better. The AMGRCop specimen, which was printed with pre-alloyed gas atomized powder, showed the Cr:Nb atomic ratio of 2 (Table 3). AMGRCop also exhibited the lowest oxygen content, likely because most of the Cr and Nb was already alloyed to Cr_2Nb prior to printing or extraction, the two suspected areas for oxide formation.

TABLE 3.—CALCULATED ELEMENT PROPORTIONS BY ATOMIC PERCENT AND AMOUNT OF Cr/Nb IN THE Cr_2Nb FOR EACH SPECIMEN

Specimen	Nb, percent	Cr, percent	O, percent	Cu, percent	Nb in Cr2Nb, percent	Cr in Cr2Nb, percent
Target	33.3	66.6	0.0	0.0	----	----
01F	58.8	15.9	8.9	16.5	9.5	70.2
01B	62.9	19.6	17.5	0.0	58.9	60.3
03J	63.8	12.3	23.8	0.0	8.6	89.2
05H	41.8	51.9	6.3	0.0	43.7	70.3
05P	36.5	53.3	10.2	0.0	62.8	86.1
05U	29.1	54.0	6.0	10.9	42.2	45.6
07AA	36.6	56.9	6.5	0.0	63.0	81.2
08C	36.8	57.4	5.8	0.0	58.0	74.3
10AJ	35.9	48.0	16.1	0.0	57.9	86.4
10AN	35.4	57.2	7.5	0.0	69.1	85.4
10AP	38.4	48.5	13.0	0.0	52.7	83.5
AMGRCop	33.9	64.3	1.8	0.0	----	----

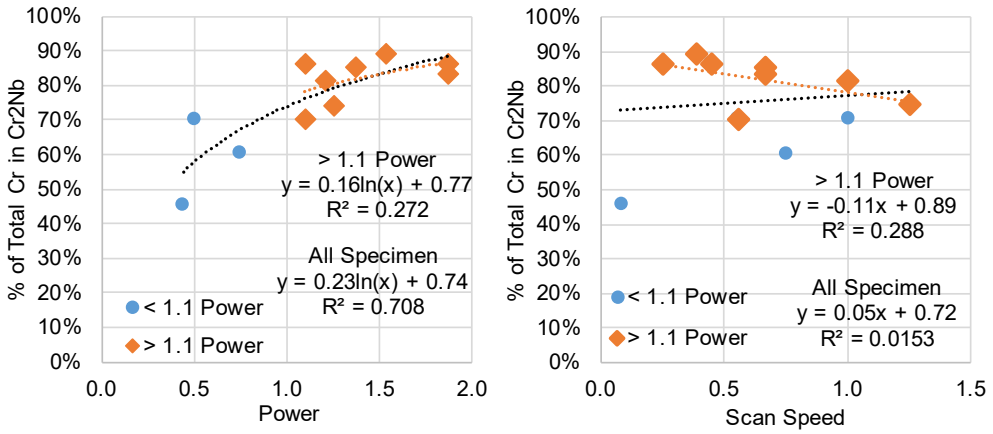

Figure 2.—Alloying effectiveness (i.e., conversion to Cr_2Nb) as compared to laser power (left) and laser scan speed (right).

Figure 3 shows that the extracted precipitates for the three specimens exhibited morphologies that were essentially indistinguishable from each other. Elemental x-ray maps, produced using EDS, were used to determine if the extracted particles were multiphase based upon gross chemical differences. Initial expectations were that particular phases, like the oxides, would be present as discrete particles. However, EDS x-ray maps shown in Figure 4 indicate little to no elemental segregation at a resolution of about 1 μm. This suggests that each precipitate contains multiple, if not necessarily all, of the phases discussed. Although only the x-ray maps from specimen 10AN are shown, specimen 10AP and AMGRCop also showed indistinguishable levels of elemental segregation. Focused ion beam sectioning and scanning transition electron microscopy analyses will be conducted to examine samples at higher resolution and validate this theory.

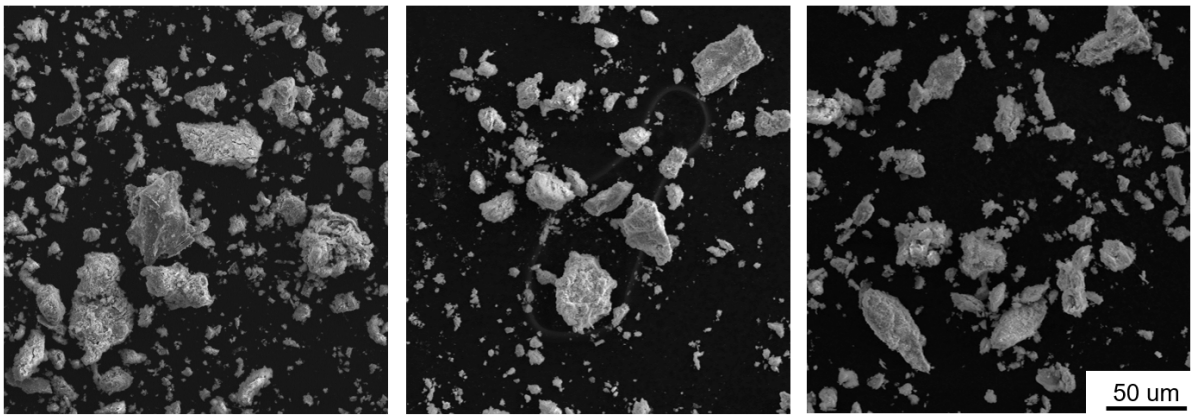

Figure 3.—Cr_2Nb Precipitate morphologies of 10AN (left), 10AP (middle), and AMGRCop (right).

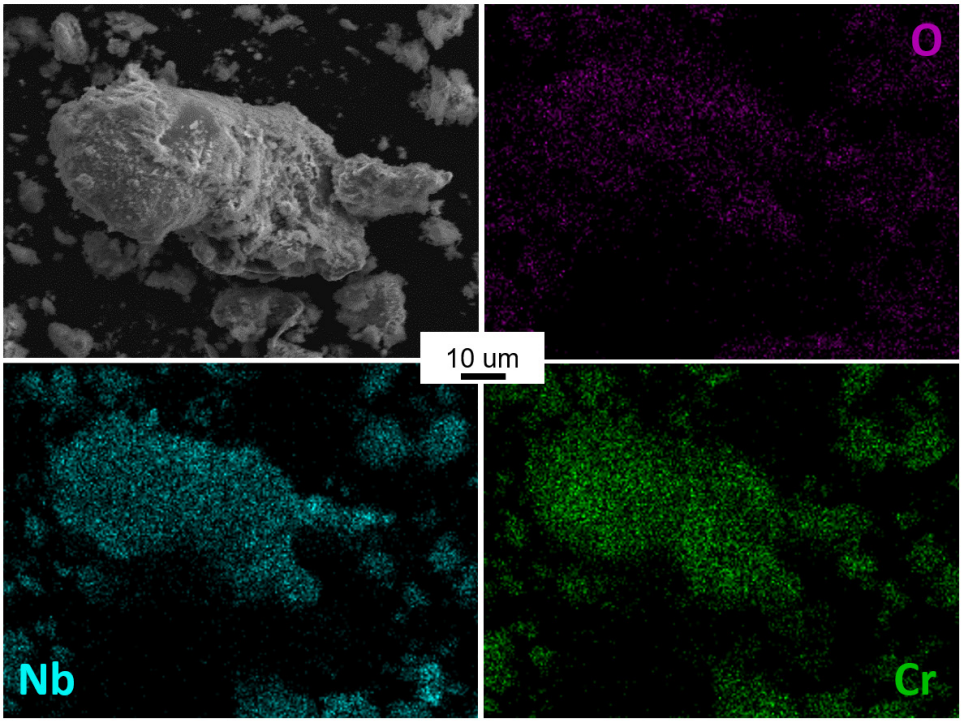

Figure 4.—EDS chemistry mapping of an in-situ alloyed Cr_2Nb particle in specimen 10AN.

Conclusions

The effects of powder preparation and LPBF parameters on the conversion of elemental powders to Cr_2Nb were investigated. These results showed that the primary variables controlling conversion were powder preparation and laser power. It is shown that the use of LPBF processing to in situ alloy dispersion strengthened alloys, such as GRCop, is possible and can be done so with a variety of printing parameters. Conversion efficiencies as high as 89% were achieved in these preliminary results. Several additional observations can be made on this work:

- Increasing surface area contact through milling and reducing the particle size of Cr and Nb was effective at improving the alloying efficiency.
- All analyzed ISGRCop samples were below a 2:1 atomic Cr:Nb ratio. The Cr deficiency is being investigated to eliminate it in future builds.
- Nb-based oxides present in the extracted precipitates indicates that either the Nb was oxidized more easily than Cr during AM, or niobium oxides were more resistant to decomposition than chromium oxides.
- Normalized laser powers greater than 1.1 produced higher alloying efficiency (i.e., formation of Cr_2Nb), although alloying efficiency appeared to asymptotically approach ~90% Cr in the Cr_2Nb phase as normalized power increased to 1.865.
- Laser scan speed influence on alloying efficiency was negligible for a normalized laser power above 1.1.
- Observed precipitate morphologies were similar regardless of oxygen content and consistent with AM GRCop-42 made from conventional gas atomized powders.
- Little to no elemental segregation in the precipitates was observed in the latest build of ISGRCop, similar to AMGRCop.

References

1. D.L. Ellis, NASA TM 2005-213566 (2005).
2. D.L. Ellis and G.M. Michal, Ultramicroscopy 30 (1988) 210–216.
3. F. Pengjun, X.Yi, L. Xinggang and C. Ya, Rare Met. Mater. and Eng. 47 (2018) 423–430.
4. B. Zheng, Y. Zhou, J. Smugeresky, J. Schoenug and E. Lavernia, Metall. Mat. Trans. A 39 (2008) 2228–2236.
5. K.G. Cooper, J.L. Lydon, M.D. LeCorre, Z.C. Jones, D.S. Scannapieco, D.L. Ellis and B.A. Lerch, NASA/TM—2018-220129 (2018).
6. Y. Gao and J. Malinzak, in PWRTEC 2012, Cangoga Park, CA, 2012.
7. J.R. Summerlin, C.L. Borgford and J.B. Ealy, Ira Remsen's Investigation of Nitric Acid, in: Chemical Demonstrations: A Sourcebook for Teachers Vol. 2, American Chemical Society, Washington D. C., 1987, pp. 4–5.
8. H.M. Rietveld, J. Appl. Cryst. 2 (1969) 65–71.
9. R.J. Hill and C.J. Howard, J. Appl. Cryst. 20 (1987) 467–474.
10. P.J. Potts, A Handbook of Silicate Rock Analysis, Springer Netherlands, 1987.